Surface solitons in chirped photonic lattices

Mario I. Molina,[1,*] Yaroslav V. Kartashov,[2] Lluis Torner,[2] and Yuri S. Kivshar[3]

[1]*Departamento de Física, Facultad de Ciencias, Universidad de Chile, Santiago, Chile*
[2]*ICFO-Institut de Ciencies Fotoniques, and Universitat Politecnica de Catalunya, Mediterranean Technology Park, 08860 Castelldefels, Barcelona, Spain*
[3]*Nonlinear Physics Centre, Research School of Physical Sciences and Engineering, Australian National University, Canberra, ACT 0200, Australia*
[*]*Corresponding author: mmolina@uchile.cl*

Received June 25, 2007; revised August 6, 2007; accepted August 7, 2007;
posted August 7, 2007 (Doc. ID 84407); published September 4, 2007

We study surface modes at the edge of a semi-infinite *chirped* photonic lattice in the framework of an effective discrete nonlinear model. We demonstrate that the lattice chirp can change dramatically the conditions for the mode localization near the surface, and we find numerically the families of discrete surface solitons in this case. Such solitons do not require any minimum power to exist provided the chirp parameter exceeds some critical value. We also analyze how the chirp modifies the interaction of a soliton with the lattice edge.

OCIS codes: 190.0190, 190.4350, 190.6135.

Electromagnetic surface waves are waves localized at the interface separating two different media [1]. Recently, the interest in the study of electromagnetic surface waves has been renewed after the first theoretical prediction [2] and subsequent experimental demonstration [3] of nonlinearity-induced self-trapping of light near the edge of a 1-D waveguide array with self-focusing nonlinearity that can lead to the formation of a discrete surface soliton. It was found that the self-trapped surface modes acquire some novel properties different from those of the discrete solitons in infinite lattices: discrete surface states can only exist above a certain threshold power and, for the same value of the power, up to two different surface modes can exist simultaneously. This can be understood as discrete optical solitons [4] localized near the edge of the lattice but experiencing a repulsive force from the effective surface [5].

A related concept of the light localization and surface gap solitons has been developed theoretically and confirmed experimentally for defocusing periodic nonlinear media [6–8]. In addition, the concept of nonlinear surface and gap solitons has been extended to the case of an interface separating two different periodic media [9–11].

In recent studies, Kartashov *et al.* [12] demonstrated that the soliton formation can be dramatically modified at the surface of chirped optical lattices. It was found that, due to combined actions of internal reflection at the interface, distributed Bragg-type reflection and focusing nonlinearity surfaces of chirped lattices become soliton attractors, in sharp contrast with the standard lattices.

In this Letter, we employ a discrete model of a chirped photonic lattice to provide a deeper physical insight into the properties of surface solitons in chirped lattices. In particular, we demonstrate that there exists a critical value of the lattice chirp for the existence of a linear localized mode at the surface such that above that critical value the surface solitons originate from the corresponding linear surface modes, and they do not require any threshold power for their existence. We study the dependence of the mode position near the surface and the critical power as a function of the lattice chirp, and also demonstrate how the lattice chirp modifies the interaction of the discrete soliton with the surface.

We consider a semi-infinite array of nonlinear waveguides. We assume that the waveguide array is chirped such that the waveguides have decreasing refraction index and increasing mutual separation as we move away from the surface (Fig. 1). As a consequence, the propagation constants of the consecutive waveguides decrease in space: $\lambda_n=\lambda_0 f(n)$, where $n=0,1,2\ldots$ and $f(n)$ is a monotonically decreasing function, with $f(0)=1$. If we assume that the change in propagation constant and mutual distance is small, the coupling strength between the consecutive waveguides will be affected in a similar way: $V_{n,n+1}=V_{n+1,n}=V_0 f(n)$. The coupled-mode equations for this waveguide system can then be written as

$$i\frac{dE_0}{d\xi}+\frac{\lambda_0}{V_0}E_0+E_1+\gamma|E_0|^2E_0=0, \quad \text{at } n=0, \tag{1}$$

$$i\frac{dE_n}{d\xi}+\left(\frac{\lambda_0}{V_0}f(n)+\gamma|E_n|^2\right)E_n+f(n)E_{n+1}+f(n-1)E_{n-1}=0, \tag{2}$$

for $n>0$, where E_n are the amplitudes of the wave-

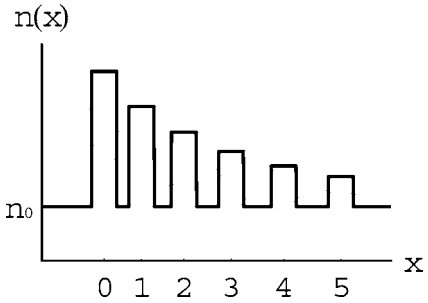

Fig. 1. Transverse profile of refraction index for a chirped array of nonlinear optical waveguides. n_0 is the linear index of the substrate.

guide modes. In deriving Eqs. (1) and (2) the electric field in the nth guide is presented as $\mathbf{e}(x,y)\mathcal{E}_n(z,t)$, where $\mathbf{e}(x,y)$ is the vectorial guided mode of the isolated waveguide and $\mathcal{E}_n$ is the mode amplitude. We use the normalization $\xi = V_0 z$, $E_n = \sqrt{\chi_{\text{eff}}/V_0}\mathcal{E}_n$, where the effective nonlinear coefficient is $\gamma\ \chi_{\text{eff}} = (\omega n_2)(cA_{\text{eff}})^{-1}$, n_2 is the nonlinear refractive index, A_{eff} is the effective mode area, and $\gamma = \pm 1$ defines focusing or defocusing nonlinearity of the waveguide material, respectively.

By looking for stationary solutions in the form, $E_n = u_n \exp[i((\lambda_0/V_0)+\beta)\xi]$, we obtain a set of nonlinear equations

$$-\beta u_0 + u_1 + \gamma |u_0|^2 u_0 = 0, \tag{3}$$

$$\Lambda_n u_n + f(n)u_{n+1} + f(n-1)u_{n-1} + \gamma |u_n|^2 u_n = 0, \tag{4}$$

where $\Lambda_n = [(\lambda_0/V_0)(f(n)-1)-\beta]$. Hereafter, we take $\lambda_0 = V_0$.

We have examined three different forms for the chirp function $f(n)$: (1) Exponential: $f(n) = \exp(-\sigma n)$, (2) Gaussian: $f(n) = \exp(-\sigma n^2)$, and (3) linear: $f(n) = 1 - \sigma n$, for $n < [1/\sigma], 0$ otherwise, where $[x]$ denotes the integer part of x. In all cases we have found the results to be qualitatively identical. For definiteness, hereafter we show the results obtained for the exponential chirp $f(n) = \exp(-\sigma n)$, but the reader should keep in mind that the results are similar for any monotonically decreasing chirp function.

First, we consider the linear case, when formally we take $\gamma = 0$ and assume weak input powers. For a fixed number of waveguides, we diagonalize the set of discrete linear equations and find solutions localized inside the array. When the chirp is increased, the mode is pushed toward the waveguide edge until, for large enough value of the chirp, the mode maximum becomes located at the edge of the array (at $n = 0$). Figures 2(a) and 2(b) show two such linear surface modes for two different chirp values. In Fig. 3(a), we show the position of the mode maximum as a function of the chirp parameter σ. The general structure is given by a series of steps of widely varying width. At small σ, the mode is located inside the chain, and a very small change in σ can change the position of the mode maximum. Closer to the surface, the steps increase in size, with the one corresponding to the position $n = 0$ being of infinite length. Thus, the linear surface mode is located at $n = 0$ for $\sigma > 0.238045$, or at $n = 1$ for $0.0557718 < \sigma < 0.238045$, or at $n = 2$ for $0.0180601 < \sigma < 0.0557718$, etc. In Fig. 3(b), we show the propagation constant for the nodeless mode as a function of the chirp parameter.

Having ascertained the general features of the surface modes at low beam powers, we consider next the nonlinear case ($\gamma \neq 0$). For given β, the stationary equations (3) and (4) are solved numerically by a multidimensional Newton–Raphson scheme. As we are interested in surface localized modes, we look for the states with maxima near the surface that decay quickly away from the array edge [see, e.g., Figs. 2(c) and 2(d) for examples of profiles of such modes]. For each nonlinear mode we perform a standard linear stability analysis.

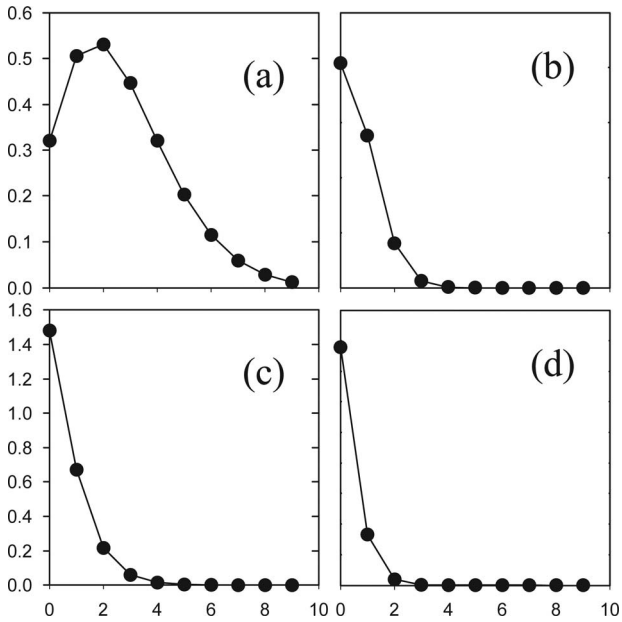

Fig. 2. (a),(b) Linear surface modes for (a) $\sigma = 0.04$ and (b) $\sigma = 0.5$. (c),(d) Nonlinear surface modes for (c) $P = 2.69$, $\beta = 2.64$, $\sigma = 0.1$; and (d) $P = 2.54$, $\beta = 2.64$, $\sigma = 0.5$ [points C and D in Fig. 4(a)]. ($N = 51$).

Figure 4(a) shows the power versus propagation constant curves of the surface mode ($n = 0$) for two values of the chirp parameter. While for small chirp a minimum power is needed to create a stable surface mode, no minimum power is required for larger chirp, and the corresponding surface states are always stable, all the way down to the linear limit $P = 0$ at the cutoff value $\beta = 0.67$. In general, one might conjecture that the presence of a monotonically decreasing chirp in the propagation constant of each waveguide and in the coupling between two neighboring guides will favor the creation of localized modes near the surface, as compared with the case of no chirp, i.e., one needs less power to effect a localized mode than in the linear case. The exact opposite behavior should happen for a monotonically increasing chirp. This is clearly evident in Fig. 4(b), where we show the minimum power required for existence

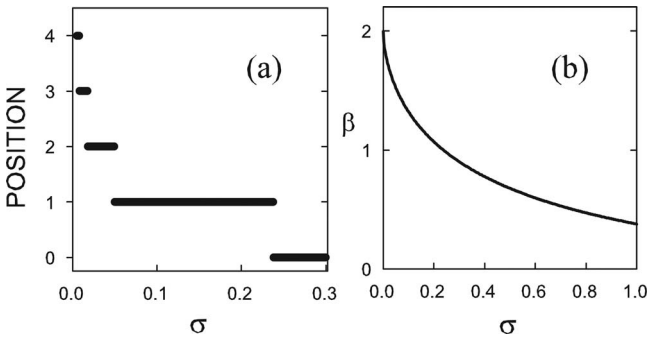

Fig. 3. (a) Position of the mode maximum in the waveguide array as a function of the chirp parameter. (b) Propagation constant of localized mode as a function of the chirp parameter ($N = 51$).

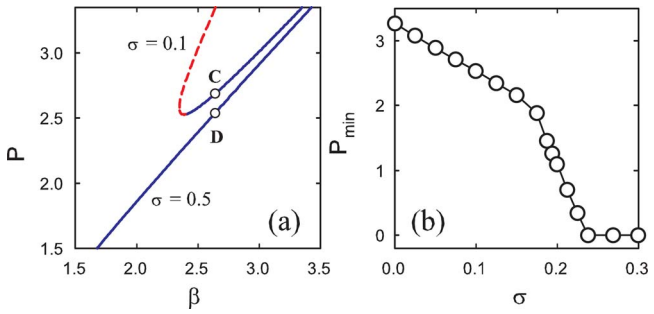

Fig. 4. (Color online) (a) Power versus propagation constant curves of surface mode for two values of the chirp parameter. Solid (dashed) curve denotes stable (unstable) mode. (b) Minimum power to create a surface mode in terms of the chirp parameter ($N=51$).

of a localized mode at the very surface as a function of the chirp. As σ is increased, the minimum power decreases. At very low power, one is in the linear regime where a surface mode can always be excited for $\sigma > 0.238$.

Finally, we examine the propagation dynamics of narrow discrete solitons in the form of a truncated sech function: $u_n = A\,\mathrm{sech}[(A/\sqrt{2})(n-n_c)]\exp[-ik(n-n_c)]$ for $|n-n_c| = 0, 1, \ldots, 4$, zero otherwise, launched toward the surface for different values of the chirp parameter. In the absence of chirp [Fig. 5(a)] the soliton approaches the surface but is repelled by it, and eventually gets self-trapped far from the surface. For small chirp [Fig. 5(b)], surface repulsion is obliterated, and the soliton gets trapped very close to the surface. Finally, at large chirp [Fig. 5(c)], the soliton remains self-trapped at the input position. This behavior can be understood from a simple analysis of

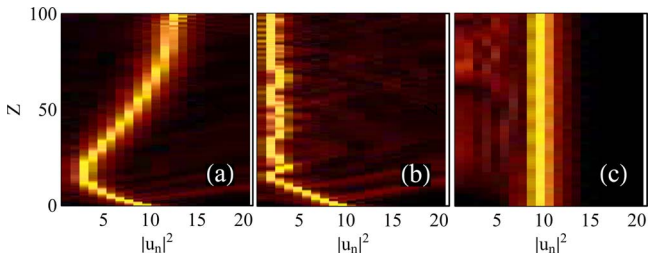

Fig. 5. (Color online) Propagation dynamics of discrete solitons launched toward the surface for various values of the chirp parameter: (a) $A=1.1, k=0.7, \sigma=0$; (b) $A=1.1, k=0.7, \sigma=0.03$; (c) $A=1.1, k=0.7, \sigma=0.5$ ($n_c=10$ and $N=101$).

Eqs. (3) and (4): At small σ, the presence of a chirp is equivalent to that of an effective force, which is responsible for the enhanced soliton mobility. At large chirp, however, there is no more effective electric field and the system becomes an effectively decoupled waveguide array, hence giving rise to complete self-trapping.

In conclusion, we have analyzed surface states at the edge of a semi-infinite chirped photonic lattice in the framework of an effective discrete model. We have demonstrated a crossover between linear surface modes and discrete surface solitons depending on the value of the lattice chirp. We believe our analysis complements the earlier studies of the chirped lattices in the continuous model, and it allows a deeper physical insight into the properties of nonlinear surface modes.

This work has been supported by Fondecyt grants 1050193 and 7050173 in Chile, and by the Australian Research Council in Australia.

References

1. P. Yeh, A. Yariv, and A. Y. Cho, Appl. Phys. Lett. **32**, 104 (1978).
2. K. G. Makris, S. Suntsov, D. N. Christodoulides, G. I. Stegeman, and A. Haché, Opt. Lett. **30**, 2466 (2005).
3. S. Suntsov, K. G. Makris, D. N. Christodoulides, G. I. Stegeman, A. Haché, R. Morandotti, H. Yang, G. Salamo, and M. Sorel, Phys. Rev. Lett. **96**, 063901 (2006).
4. Yu. S. Kivshar and G. P. Agrawal, *Optical Solitons: From Fibers to Photonic Crystals* (Academic, 2003).
5. M. Molina, R. Vicencio, and Yu. S. Kivshar, Opt. Lett. **31**, 1693 (2006).
6. Ya. V. Kartashov, V. V. Vysloukh, and L. Torner, Phys. Rev. Lett. **96**, 073901 (2006).
7. C. R. Rosberg, D. N. Neshev, W. Krolikowski, A. Mitchell, R. A. Vicencio, M. I. Molina, and Yu. S. Kivshar, Phys. Rev. Lett. **97**, 083901 (2006).
8. E. Smirnov, M. Stepic, C. E. Ruter, D. Kip, and V. Shandarov, Opt. Lett. **31**, 2338 (2006).
9. K. G. Makris, J. Hudock, D. N. Christodoulides, G. I. Stegeman, O. Manela, and M. Segev, Opt. Lett. **31**, 2774 (2006).
10. K. Motzek, A. A. Sukhorukov, and Yu. S. Kivshar, Opt. Express **14**, 9873 (2006).
11. M. I. Molina and Yu. S. Kivshar, Phys. Lett. A **362**, 280 (2007).
12. Ya. V. Kartashov, V. A. Vysloukh, and L. Torner, Phys. Rev. A **76**, 013831 (2007).